Nanoscale texture development of C-S-H gel: A computational model for nucleation and growth

R. González-Teresa, J. S. Dolado, A. Ayuela, and Jean-Christophe Gimel

---

Articles you may be interested in

Cause of the fragile-to-strong transition observed in water confined in C-S-H gel
J. Chem. Phys. **139**, 164714 (2013); 10.1063/1.4826638

Computer simulation study of the phase behavior and structural relaxation in a gel-former modeled by three-body interactions
J. Chem. Phys. **134**, 164506 (2011); 10.1063/1.3578176

Effect of hydration on the dielectric properties of C-S-H gel
J. Chem. Phys. **134**, 034509 (2011); 10.1063/1.3521481

Diamond nucleation on iridium buffer layers and subsequent textured growth: A route for the realization of single-crystal diamond films
Appl. Phys. Lett. **78**, 192 (2001); 10.1063/1.1337648

Computer simulation studies of diffusion in gels: Model structures
J. Chem. Phys. **107**, 9221 (1997); 10.1063/1.475214

CrossMark
click for updates

Nanoscale texture development of C-S-H gel: A computational model for nucleation and growth

R. González-Teresa,[1] J. S. Dolado,[1,a)] A. Ayuela,[2] and Jean-Christophe Gimel[3]

[1]*Tecnalia Research and Innovation, Derio, Spain*
[2]*Centro de Física de Materiales CFM-MPC, Centro Mixto CSIC-UPV/EHU,*
and Donostia Internacional Physics Center, San Sebastián, Spain
[3]*LUNAM Université, Université du Maine, IMMM–UMR CNRS 6283, Département Polymères*
Colloïdes et Interfaces, av. O. Messiaen, 72085 Le Mans Cedex 9, France

The development of C-S-H (Calcium-Silicate-Hydrate) gels during cement hydration is often investigated by nucleation and growth models which fit reasonably well with the calorimetric measurements but predict hydration degrees which grossly exceed the experimental values. Here, a computational model is presented which explicitly considers the intrinsic nanoparticulate nature of C-S-H gel. Based on a nucleation and growth algorithm the model reproduces the experimental calorimetric and hydration degree measurements without invoking to any diffusion mechanism. The model also suggests that the peak in the calorimetric curves can be ascribed to the percolation point of the hydrates themselves within the interstitial pore volume. © 2013 AIP Publishing LLC. [http://dx.doi.org/10.1063/1.4838396]

Detailed knowledge of the underlying mechanism for the hydration of cementitious materials is needed in order to improve their manufacturing. During hydration, the cohesion of cement-based materials[1] is due to the precipitation of Calcium Silicate Hydrates, the so called C-S-H gel, where in cement notation $C = CaO$, $S = SiO_2$, and $H = H_2O$. The most important phase in ordinary Portland cement is a tricalcium silicate, either called alite or C_3S.[2,3] The hydration process of C_3S is studied using isothermal calorimetry.[4,5] The overall progress of hydration is divided into four stages as seen in Figure 1. The first and the second stages correspond to the initial and induction periods, respectively, where alite rapidly dissolves from cement grains and a period of low activity is followed. The stage III, called the acceleration period, is related to nucleation and growth of the nanoparticles of C-S-H gel in the space between cement grains. In the last stage IV, in the deceleration period, the rate of hydration decreases and is generally assumed to be controlled by diffusion of these nanoparticles.[6] Our topic is the modeling of these third and fourth stages of alite hydration.

Several nucleation and growth models were recently developed to explain the third and fourth stages of tricalcium silicate hydration. The Avrami model[7,8] considered that an isothermal phase transformation occurs within a fixed volume by nucleation and growth. The nucleation is spatially random, and the growth is linear in any direction. Each region of transformed phase is thus spherical. With this model, it is possible to reproduce the calorimetry curve before the peak in the region III, but in the region IV after the peak the rate given by the model deviates from the experiment. As pointed by Thomas,[9] the description of the hydration rate of C_3S was substantially improved by using a modified form of the boundary nucleation and growth (BNG) model developed by Cahn.[10] In this case, the nuclei

aggregate on planar boundaries that are randomly distributed within the pore volume between cement grains, which leads to an improved fit to experiment after the peak. However, the BNG model predicts a hydrated volume fraction at the peak that is too high in comparison with experiments.[11] This difference might result from the BNG model neglecting confinement in the pores. Then, several nucleation and growth models were reviewed by Scherer,[11] focusing especially on those that describe growth confined within boundaries. They are hereafter called confined boundary nucleation and growth (CBNG) models. By taking into account the confinement within the cement grains, the volume occupied by the hydrates still overestimates the experimental observation. This can be easily observed by comparing the degree of hydration (α). It accounts for the amount of cement consumed and, therefore, it is proportional to the hydrated volume fraction. The degree of hydration at the peak drops from ∼0.5 in Avrami and BNG models to about ∼0.25 (Ref. 11) when the growth is restricted to cylindrical pores. This last value still differs considerably from the experimental value of 0.071 ± 0.007.[12] The review concluded that the confinement is insufficient to capture the essential features of the process and that other factors must be invoked. This discrepancy was rationalized in Ref. 11 as the consequence of a dendritic growth followed by in-filling, something similarly was suggested by Bishnoi and Scrivener.[13] These recent works pointed to the presence of a certain texture in the hydrate and casted some doubt on the real diffusive origin of the deceleration period.[9,11,13]

Much recent work focuses on the nanoscale of C-S-H gel and expands bottom up into larger scales. Numerous experimental[14] and computational[15] studies agree that C-S-H nanotexture can be viewed as a mixture of tobermorite and jennite structures in which these layered species show multiple imperfections, but the nanoscopic short-ordering structure (1–5 nm) of C-S-H gel remains elusive.[16] At larger scales, C-S-H gel is adequately described as granular.

a)Author to whom correspondence should be addressed. Electronic mail: jorge.dolado@tecnalia.com. Tel.: +34 607 40 33 13.
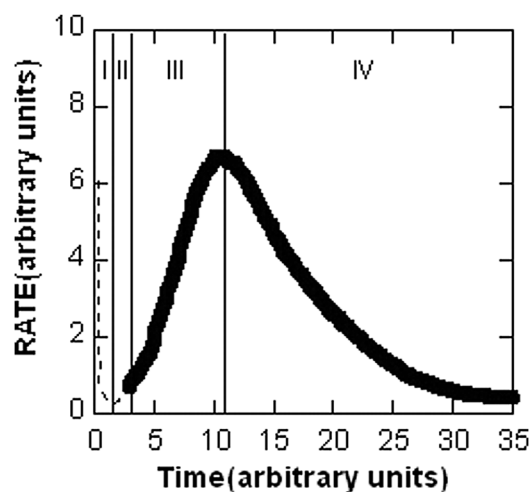
FIG. 1. Typical heat evolution curve for the hydration of tricalcium silicate. Roman numbers indicate different stages. This work focuses on stages III and IV.

Different experimental[17,18] and computational works[19] have shown lately that there are 4–5 nm features in the structure of C-S-H gel. These features are usually interpreted in colloidal models[20] as the basic building blocks of C-S-H. In essence, these colloidal models suggest that the morphology of C-S-H arises from the aggregation of these 4–5 nm sized particles, giving rise to a colloidal type of gel.[21,22] At larger scales, nucleation and growth models have thus to take into account implicitly the intrinsic nanoparticulate nature of the C-S-H.

In this work, we propose a computational model to simulate the formation of C-S-H through a random sequential addition (RSA)[23] of the nano-colloid C-S-H nuclei, which grow hierarchically. The model captures the growth of C-S-H and its evolving texture on an equal footing, and accounts simultaneously for the calorimetric and hydration degree results.

In essence, we develop a computational scheme for the nucleation and growth of the 5 nm sized colloid C-S-H units in the interstices between cement grains, as seen schematically in Fig. 2. For our purpose, the nucleation and growth confined between boundaries is assumed to be insensitive to
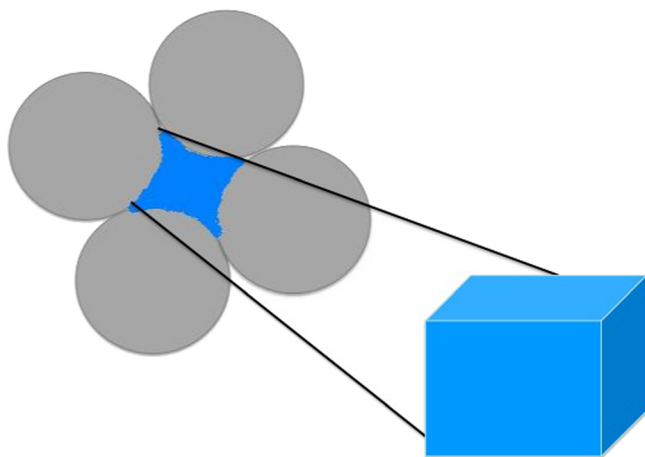

FIG. 2. Scheme for pores space between cement grains. The shape of the pores space is approximated by a cubic box in which the simulations are performed.[11]

details of the pore shape,[11] and the pore space is approximated by a cubic box for simplicity. For the box size, a characteristic length $L \sim 50$ nm was taken for the pore space. This length results from consideration of the mean nearest-neighbour distance[23] between randomly positioned cement particles with typical diameter of few microns and a packing volume fraction around 0.5.[24]

The evolution of C-S-H texture is simulated by a process which combines rate-dependent nucleation with a hierarchical growth mechanism. The nucleation is simulated by random insertion of 5 nm sized C-S-H units in the simulation box. These nuclei appear in time according to the relation

$$\eta(t) = \eta_0(1 - e^{-t/\tau}), \tag{1}$$

where η(t) is the density of nuclei present inside the box at simulation time t and η_0 is the target final density of nuclei. The value of τ defines a characteristic time for the appearance of nuclei inside the box. A hard sphere potential is used to describe the interaction of the fresh C-S-H nuclei with the already existing C-S-H particles, regardless of whether they are grown particles or bare nuclei. During nucleation, the new C-S-H units are randomly placed without overlapping others, a filling that follows the non equilibrium physics of RSA processes.[25] On the other hand, the growth around each nucleus is modeled by a hierarchical packing scheme,[26,27] which gives textural details in agreement with the pictures of C-S-H gel as drawn by Jennings' models.[20,28] Clusters grow by forming successive layers of C-S-H units around previous ones, starting from the C-S-H nuclei. Each cluster grows following an "Avramian growth," in the sense that the radius of each cluster grows linearly with time. Excluded volume constrains have been superimposed to the growth protocol. Particles are randomly inserted in contact with at least one of the earlier deposited layers, while avoiding overlap with the rest. When a layer is formed around a randomly chosen nuclei the simulation time step is increased by $1/\eta$(t). This time step is scaled according to the number of added C-S-H nuclei so that all the growing C-S-H clusters have the same opportunity to growth. Because we arbitrary set the growth time step to one, the characteristic time τ defines also the rate between nucleation and growth processes. We alternate these nucleation and growth processes until there is no space left. Different structures and textures can be grown by changing the parameters η_0 and τ. This pair of parameters fully specifies a configuration of C-S-H gel. Simulations are repeated at least one hundred times to get meaningful statistical averages.

A typical curve obtained from our simulations for the rate of growth versus time is plotted in Fig. 3 (left panel). The particular system shown in Fig. 3 corresponds to the one with a density $\eta_0 = 1.088 \times 10^{-3}$ seeds/nm^3 and a characteristic nucleation time $\tau = 1$. As can be seen the rate increases up to a maximum, where it starts to fall slowly decelerating. In all our simulation, we find that the peak corresponds to the percolation of nanoparticles in the hydrate between pores. Some snapshots taken during the simulation are also presented in the right panel of Figure 3, corresponding to the (a)–(f) points in the plot. The simulation starts with a certain number of nuclei inside the simulation box following
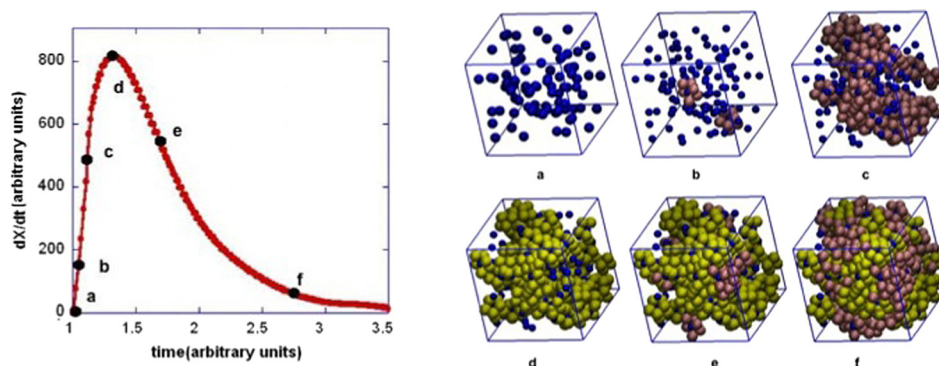
FIG. 3. Typical curve for rate of growth versus time obtained from the simulations. The particular system shown corresponds to the one with $\eta_0 = 1.1 \times 10^{-3}$ nm^{-3} and $\tau = 1$. Black dots correspond to the (a)–(f) snapshots taken during the simulation. Nuclei are coloured as blue spheres. During growth, the C-S-H formed by linking nanoparticles is coloured with pink spheres. When the percolation takes place (d) the percolated C-S-H skeleton is coloured in yellow. After percolation C-S-H continues growing. To illustrate this point, the new C-S-H particles that appear after percolation are coloured in pink. (panels e and f).

Eq. (1). Snapshot (a) shows the initial nucleation seeds. After a time, the C-S-H nanoparticles start to grow around the nucleation sites, as given in the (b) and (c) panels. The formation of C-S-H continues until all the nanoparticles percolate in three dimensions. The percolated structure shown in the (d) panel is coloured differently. This point corresponds to the maximum in the hydration rate versus time graph. Note that the percolation of the whole cement paste including cement grains is known to occur much earlier, at the initial setting point.[24] The initial setting defines the starting point of the acceleration period (Stage III) and is generally rationalized as the point at which a negligible amount of hydration product is capable of linking the clinker particles, leading to the formation of a continuum and elastic porous skeleton. Our simulations reveal that there is a second percolation process by which the hydrates themselves percolate the volume of the mentioned continuous pore skeleton and that this percolation process can be ascribed to the peak in the rate of C-S-H formation. This result justifies the naming of the peak in the calorimetry curve as the final setting.[29] After the peak, the C-S-H clusters continue growing new C-S-H particles on their surfaces and new C-S-H nuclei might eventually appear (as shown in the (e) panel). This nucleation and growth process continues until there is space for no more C-S-H particle (snapshot shown in the (f) panel).

A comparison with the experiment is possible by employing τ and η_0 as fitting parameters and rescaling the theoretical predictions to the experimental ones. To compare our model to the calorimetric measurements, the simulation time and the rate of occupied volume $dX(t)/dt$ have been multiplied by appropriate scaling factors so as to make the experimental and theoretical values coincide at the peak. A detailed study about how these parameters can be used to fit different cement systems is beyond the scope of this work, and will be presented elsewhere. Here, we focus attention on the hydration of tricalcium silicate and compare the results of the simulation with the observed calorimetric curve.[4] The best fit to experiments is for simulation parameters $\eta_0 = 4.0 \times 10^{-3}$ seeds/nm^3 and $\tau = 1$, and is presented in Figure 4. The calculated rate of heat versus time is denoted by the small black dots and experiments by open-red marks. Our simulations are in excellent agreement with the experiments. The results of fitting Avrami and BNG models to

experiments are shown as dashed and solid lines, respectively. As a measure of the degree to which models describe the experimental data, Thomas[9] defined the ratio t_{dev}/t_{peak}, where t_{dev} is the time when the fit deviates from the data, and t_{peak} is the time at the peak. For Avrami and BNG models, the t_{dev}/t_{peak} ratios are about 1.23 and 1.86, respectively, whereas our model fits the experimental data in the whole analysed range. This agreement suggests that our nucleation and growth scheme captures the kinetics of C-S-H formation. This finding supports previous works,[9,11,13] which cast doubt on the "diffusive" origin of the deceleration regime.

While accounting for the calorimetric profiles is a basic requirement of the models, the real challenge lies on explaining the low hydration degrees (α) found experimentally at the calorimetry peak.[12] Note that there is direct relationship between X and α[11]

$$\alpha = X \frac{\rho_{CSH} R_{wc} \rho_c / \rho_w}{\rho_c \left(1 + \frac{m_w}{m_c}\right) - \rho_{CSH}}, \qquad (2)$$
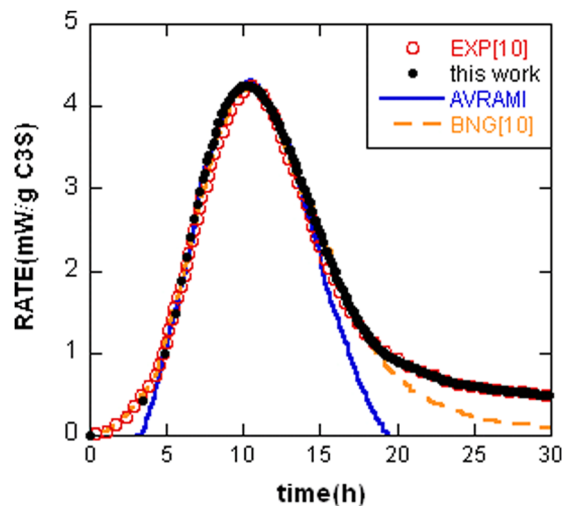

FIG. 4. Rate of occupied volume versus time fitted to alite. Black dots denote our simulations corresponding to alite with a density $\eta_0 = 4.0 \times 10^{-3}$ seeds/nm^3 and a nucleation characteristic time $\tau = 1$. The experimental calorimetric curve[9] for the hydration is the red line. Are also plotted in blue solid and orange dashed lines results for the Avrami model[8] and the BNG model,[9] respectively.

where R_{wc} (=0.5 in this study) is the water/cement mass ratio, m_w/m_c (~0.45) is the average water/cement mass ratio of the hydration products, ρ_c (3.15 g/cm^3) is the density of cement particles (alite in this study), ρ_w (1 g/cm^3) is the density of water, and ρ_{CSH} stands for the average density of C-S-H gel. It is worth noting that our model naturally accounts for a progressive densification of C-S-H gel and the average density of C-S-H is obtained from

$$\rho_{CSH}(t) = X(t)\rho_P + (1 - X(t))\rho_w, \qquad (3)$$

where ρ_P is the density of the dried colloid unit (2.8 g/cm^3).[28] The presence of C–S–H with increasing density is not explicitly present in previous nucleation and growth models, where the average density of C-S-H is usually fixed to a value of 2.0 g/cm^3. Interestingly, this densification process agrees well with the microstructural picture drawn in Ref. 13 for the early hydration product formation.

In Fig. 5 are plotted the rate of occupied volume (dX/dt) as a function of the volume transformed (X) for the models (left panel). To facilitate comparison with experiment, the rate is also shown in terms of the degree of hydration, α (right panel). Fig. 5 shows that the values obtained at the peak for the Avrami model are $X \sim 0.5$ and $\alpha \sim 0.44$, corresponding values for the BNG model are $X \sim 0.4$ and $\alpha \sim 0.36$. These grossly overestimate the experimental value of $\alpha \sim 0.071$,[12] which is shown in the figure by a vertical dashed line. For the sake of comparison Fig. 5 also shows the predictions of a CBNG model employed in Ref. 11 for fitting the chemical shrinkage data of Class H cement at 25 °C, $R_{wc} = 0.35$. As can be seen, the confinement allows a drop in the values to $X \sim 0.23$ and $\alpha \sim 0.2$, but they are still far away from the experimental value. Finally, our simulations predict that $X = 0.1 \pm 0.06$ and $\alpha \sim 0.075$, values which agree extremely well with the experiments.

We note that according to our simulations, the volume transformed at the peak corresponds to the volume when the pore space percolates. The low value obtained for this percolation threshold ($X = 0.1$) is in good agreement with the ones found using RSA models.[23] The average density of the C-S-H gel at the peak, ρ_{CSH}(peak), is obtained from Eq. (3). Our model predicts the average value ρ_{CSH}(peak) = 1.2 g/cm^3, density which matches extremely well with the value

obtained by Bishnoi and Scrivener (1.19 g/cm^3) when fitting experiments on alite with μic model.[30]

While current model concurrently provides a satisfactory explanation of the early C-S-H formation, the value of the maximum occupation fraction for our model ($X_{max} \sim 0.4$) differs from the one found in mature cement pastes, where C-S-H gel is known to reach values consistent with random close packing ($X_{max} \sim 0.64$). Several factors could account for this difference. First, our model follows RSA scheme where the C-S-H clusters grow frozen at their initial positions. The so formed systems are not in an equilibrium state. Allowing the C-S-H clusters to move and explore the sample configuration would free space at longer times than in these simulations and allow further growth, so that the value of the maximum volume fraction would increase. It is worth noting that our simulations indicate that the characteristic time required for the system to relax and reach equilibrium should be much longer than the characteristic times that govern the early stages of C-S-H growth, i.e., the nucleation and growth characteristic times. Second, the growth proposed in our model is isotropic in the sense that the radius of each cluster (R_c) grows linearly with time. Introducing anisotropy during growth would allow the maximum volume fraction to increase.[31] The effects of anisotropy can easily be included in the model by assigning preferential growth directions to each C-S-H cluster; i.e., the sizes along the preferential directions ($R_\parallel$) and the sizes along the perpendicular ones ($R_\perp$) grow at different rates. A preliminary study has been carried out. The simulations confirm that a slight anisotropy can increase the packing efficiency. Finally, other effects such as creep and shrinkage should also be taken into account. They rightly belong to processes that take place over time scales much longer than these presented here, and are beyond the scope of this work.

In summary, a nucleation and growth model has been developed based on a spatially random but rate dependent sequential addition of (mono-sized) nano-colloid units which grow hierarchically. The model has been applied to study the early hydration of alite and has allowed us to include the texture at the nanoscale of C-S-H gel. By an appropriate election of the simulation parameters ($\eta_0 = 4.0 \times 10^{-3}$ seeds/nm^3 and $\tau = 1$), the simulated rate of C-S-H growth matches extremely well with the experimental calorimetric curve of alite in the whole measured time interval. It should be noted that although the model is not diffusive, the region after the peak is modeled with great accuracy. Furthermore, the value for the degree of hydration at the peak was found to be about 0.075, in fairly good agreement with the experimental value, 0.071.[12] This low occupation fraction at the peak, largely overestimated by previous models, has found to correspond to the point where the growing C-S-H structure percolates the pore interstitial volume. At this point, the value for the predicted mean density of the formed gel is ρ_{CSH}(peak) = 1.2 g/cm^3, also consistent with Ref. 30. Developed to describe the early growth stages, the model does not capture the physics of the hydration process at longer times and its concurrent C-S-H densification. This will surely require a detailed analysis of the relaxation processes of the C-S-H colloids. It is clear that an in-depth work is needed in such a direction.
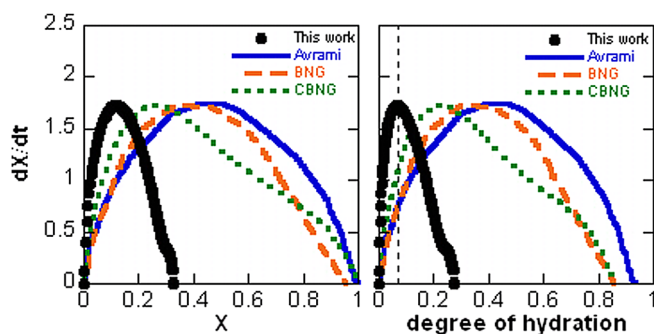

FIG. 5. Rate of occupied volume fraction versus the hydrated volume X (left panel) and the degree of hydration (right panel). Our simulations are given with solid points. The values for the Avrami,[8] BNG,[9] and CBNG[11] models are also given with a solid, dashed, and dotted line, respectively. The experimental degree of hydration at the peak (0.071) is shown by a vertical dashed line.

[1]J. W. Bullard, H. M. Jennings, R. A. Livingston, A. Nonat, G. W. Scherer, J. S. Schweitzer, K. L. Scrivener, and J. J. Thomas, Cem. Concr. Res. **41**, 1208 (2011).

[2]I. G. Richardson, Cem. Concr. Compos. **22**(2), 97 (2000).

[3]H. F. Taylor, *Cement Chemistry*, 2nd ed. (Thomas Telford Publishing, London, 1997).

[4]E. M. Gartner, J. F. Young, D. A. Damidot, and I. Jawed, "Hydration of portland cement," in *Structure and Performance of Cements*, edited by J. Bensted and P. Barnes (Spon Press, London, 2002), pp. 57–113.

[5]R. Kondo and M. Daimon, J. Am. Ceram. Soc. **52**, 503 (1969).

[6]R. B. Williamson, Prog. Mater. Sci. **15**, 189 (1972).

[7]M. Avrami, J. Chem. Phys. **7**, 1103 (1939).

[8]M. Avrami, J. Chem. Phys. **8**, 212 (1940).

[9]J. J. Thomas, J. Am. Ceram. Soc. **90**(10), 3282 (2007).

[10]J. W. Cahn, Acta. Metall. **4**, 449 (1956).

[11]G. W. Scherer, Cem. Concr. Res. **42**, 1252 (2012).

[12]J. Zhang, E. A. Weissinger, S. Peethamparan, and G. W. Scherer, Cem. Concr. Res. **40**, 1023 (2010).

[13]S. Bishnoi and K. L. Scrivener, Cem. Concr. Res. **39**, 849 (2009).

[14]V. S. Ramachandran and J. J. Beaudoin, *Handbook of Analytical Techniques in Concrete* (William Andrew Publishing, Norwich, New York, 2001).

[15]A. Ayuela, J. S. Dolado, I. Campillo, Y. R. de Miguel, E. Erkizia, D. Sánchez-Portal, A. Rubio, A. Porro, and P. M. Echenique, J. Chem. Phys. **127**, 164710 (2007).

[16]P. Rejmak, J. S. Dolado, M. J. Stott, and A. Ayuela, J. Phys. Chem. C **116**, 9755 (2012).

[17]A. J. Allen, J. J. Thomas, and H. Jennings, Nature Mater. **6**, 311 (2007).

[18]J. J. Thomas, H. M. Jennings, and A. J. Allen, Cem. Concr. Res. **28**, 897 (1998).

[19]J. S. Dolado, M. Griebel, J. Hamaekers, and F. Heber, J. Mater. Chem. **21**, 4445 (2011).

[20]H. Jennings, Cem. Concr. Res. **38**, 275–289 (2008).

[21]G. W. Scherer, Cem. Concr. Res. **29**, 1149 (1999).

[22]E. Masoero, E. Del Gado, R. J.-M. Pellenq, F.-J. Ulm, and S. Yip, Phys. Rev. Lett. **109**, 155503 (2012).

[23]S. Torquato, *Random Heterogeneous Materials. Microstructure and Macroscopic Properties* (Springer, New York, 2002).

[24]G. W. Scherer, J. Zhang, J. Quintanilla, and S. Torquato, Cem. Concr. Res. **42**, 665 (2012).

[25]B. Widom, J. Chem. Phys. **44**, 3888 (1966).

[26]V. Morales-Flórez and F. Brunet, Mol. Simul. **35**, 1001 (2009).

[27]R. González-Teresa, V. Morales-Florez, H. Manzano, and J. S. Dolado, Mater. Constr. **60**, 7 (2010).

[28]H. Jennings, Cem. Concr. Res. **30**, 101 (2000).

[29]Z. Sun, T. Voigt, and S. P. Shah, Cem. Concr. Res. **36**, 278 (2006).

[30]S. Bishnoi and K. L. Scrivener, Cem. Concr. Res. **39**, 266 (2009).

[31]A. Donev, I. Cisse, D. Sachs, E. A. Variano, F. H. Stillinger, R. Conelly, S. Torquato, and P. M. Chaikin, Science **303**, 990 (2004).